Simulation Modelling Practice and Theory 138 (2025) 103036

Contents lists available at ScienceDirect

Simulation Modelling Practice and Theory

journal homepage: www.elsevier.com/locate/simpat

Do the sparser access points have less impact on arterial traffic? A microscopic simulation-based study

Jing Zhao [a,b,*], Yulan Xia [a], Chaojun Wang [a], Jairus Odawa [c]

[a] *Department of Traffic Engineering, University of Shanghai for Science and Technology, Shanghai, PR China*
[b] *Smart Urban Mobility Institute, University of Shanghai for Science and Technology, Shanghai, PR China*
[c] *Department of Information Technology, Masinde Muliro University of Science and Technology, Kenya*

ARTICLE INFO

Keywords:
Access points
Microscopic traffic simulation
Traffic flow
Capacity

ABSTRACT

A dynamic microscopic traffic flow simulation within a ring arterial context was developed to investigate the effects of access point spacing on urban arterial flow under a right-in-right-out access management system. The microscopic traffic flow model, centered on car-following and lane-changing behaviors, was established based on vehicle interactions. The car-following aspect encompasses free driving, car-following behavior, and deceleration and braking states while lane-changing considerations include decision-making and acceptable gap assessment. Experimental scenarios account for arterial traffic density, access traffic demand intensity, average access point spacing, and variation coefficient of access point spacing. The traffic flow and speeds within the ring arterial were evaluated across 5040 operational conditions (equating to 5880 simulation hours). The traffic flow trends and speed variations with density across different access spacing scenarios were analyzed. We made an intriguing discovery: the impact on arterial traffic flow increases with larger average access point spacing, challenging conventional traffic planning recommendations that advocate for greater spacing. Additionally, access traffic minimally affects the overall arterial flow when arterial traffic volume is low. By highlighting these critical insights, this study introduces novel considerations for designing and managing access points.

1. Introduction

Vehicles entering and exiting at access points along residential areas, companies, or parking areas can significantly impact the operation of urban roads. However, these access points are essential for connecting lots to the roadway. Over the past decades, studies have been conducted on managing access traffic [11]. Among these studies, it is generally recognized that for allowing left-in-left-out access, the impact on arterial traffic flow is lower when the traffic density at access points is lower and the spacing is greater. Therefore, in traffic planning and design, strictly limiting the number of access points in a neighborhood is imperative. However, if access traffic is managed by allowing only right-in-right-out movements, does the principle still hold that the sparser the access points are, the less impact the efficiency of road traffic operation will have? This question prompts a deeper investigation into the relationship between access point density and traffic flow efficiency.

Access traffic can be observed at entry and exit points for side roads, companies, alleys, residential areas, and commercial districts [44]. Strategies for managing access traffic encompass location selection, spacing limitation, geometric design, and operation control

* Corresponding author.
E-mail address: jing_zhao_traffic@163.com (J. Zhao).

https://doi.org/10.1016/j.simpat.2024.103036
Received 13 June 2024; Received in revised form 8 October 2024; Accepted 4 November 2024
Available online 6 November 2024

[10,31,45]. Numerous studies have highlighted the disruptive impact of inappropriate access spacing on traffic flow [49]. Zhang and Zhou [47] noted that drivers may inadvertently travel in the wrong direction due to factors such as a closely spaced median opening, inadequate front access control, and absence of package road connections, potentially leading to accidents [34]. Schultz et al. [33] explored the relationship between access factors like segment length, signal spacing, access category, access density, and crashes, revealing a significant link between the spacing and density of access points in commercial areas and the total number of crashes and crash rates. Based on this, Huang et al. [16] introduced the concept of access density, defined as the sum of access weights of different access points on a road section divided by the length of the road section, further reinforcing the positive correlation between access density and crash rates [5,14,26]. Therefore, from a management perspective, controlling access traffic plays a pivotal role in improving the safety and efficiency of urban roads. Access management primarily regulates access spacing and vehicle turning to mitigate potential risks and enhance overall traffic operations.

In theoretical studies concerning access spacing, the primary basis for determining access spacing is the impact of road traffic capacity and speed. Zhou et al. [53] utilized Corsim to assess the capacity and safety advantages of access settings in highway interchange adjacent areas, highlighting that the optimal spacing to expand the limited access right-of-way at interchange locations is 400m. Dixon and Brown [9] observed that driveway activities typically involve deceleration maneuvers rather than full stops, suggesting that establishing the minimum spacing between driveways based on perception-reaction time alone may not be appropriate. To address this issue, Gattis et al. [11] proposed a minimum spacing of 200 ft between vehicles turning right from an access connection onto the arterial and the subsequent connection on the same side of the arterial, taking into account perception-reaction time, crossing time, and buffer time to prevent collisions. Brewer et al. [6] synthesized existing policies, literature, and guidelines to determine driveway and intersection spacing for rural highways at various design speeds. Chu et al. [7] analyzed the impacts of speed limits, traffic volume, and minimum access spacing on traffic safety operations. The findings indicated that speed limits and traffic volume are the primary factors influencing the safety of access points.

Regarding practical experiences with access spacing, various regions have established normative values for access spacing [42]. The Highway Capacity Manual (HCM) recommends different standards for access point spacing based on the region: 20 access points per mile (approximately every 160 m) in remote areas; 10 to 20 access points per mile (roughly every 80 m to 160 m) in urban suburbs; and 21 access points per mile (about every 76 m) or more in urban core areas [43].

The aforementioned studies have primarily focused on access management methods that manipulate the spacing settings for access points. However, the turning behavior of vehicles is also a crucial factor influencing traffic flow on roadways. Specifically, the presence of a raised median can significantly reduce the number of traffic conflicts compared to a two-way left-turn lane with the same traffic volume [19,24,50]. Additionally, as arterial traffic volume increases, implementing right turns with U-turns at median openings can decrease traffic delays compared to direct left turns [46]. Gluck et al. [13] determined deceleration lane lengths and access separation distances at various operating speeds and levels of right-turn traffic. Khan et al. [18] conducted a comparative analysis involving different access management strategies, such as allowing direct left turns at all driveways, restricting driveway traffic to right-in–right-out movements with U-turns permitted at signalized intersections, implementing peak-hour restrictions on direct left turns at driveways, and dynamically restricting driveways to right-in–right-out access. Their findings indicated that transitioning driveway entrances from fully open to right-in–right-out based on dynamic traffic restrictions can enhance traffic operations.

Furthermore, other researchers have approached access management from the standpoint of integration and optimization. Tenekeci et al. [39] introduced an integrated traffic management strategy that combined microprocessor-optimized vehicle actuation signals with ramp metering and access management. This approach led to a 38 % improvement in the average speed of the arterial road. Medina et al. [25] devised an optimal access management technique using model predictive control to minimize vehicle dwell time at intersections, thereby enhancing the traffic throughput of the intersection.

Most studies above analyze individual access points' impact on arterial traffic efficiency. They typically consider the flow rate of a single access point as an input and conclude that a lower density of access points (larger spacing) has a lesser impact on urban arterial traffic flow. However, in practical scenarios, the total demand of access traffic along the arterial remains constant. Reducing the density of access points can have both positive and negative effects on arterial traffic flow. On the positive side, increasing the spacing between access points reduces the number of access traffic interactions affecting arterial traffic flow. Conversely, on the negative side, the traffic volume at individual access points increases, intensifying the impact of each access point on arterial road traffic flow. Therefore, with a fixed total demand for access traffic, it may not be accurate to conclude that lower density will necessarily lead to a reduced impact on urban arterial traffic flow.

In this study, we aim to investigate the impact of access spacing under right-in-right-out management on urban arterial traffic flow through microscopic traffic dynamics simulation. The contribution is twofold: (1) We develop a microscopic traffic flow simulation model as a ring road, enabling the simulation of urban arterial traffic flow operations under various access arrangement conditions. (2) We consider four key influencing factors: arterial traffic density, traffic demand intensity of access, average spacing of access points, and the coefficient of variation of access spacing. By conducting a large-scale simulation involving 5040 different conditions and spanning 5880 h, we aim to elucidate how access traffic influences arterial traffic capacity.

The article is organized as follows. Section 2 establishes the framework of the microscopic traffic simulation. Section 3 outlines the detailed microscopic traffic flow model, which describes the interactions of the vehicles. Section 4 introduces the simulation experiment design. Section 5 analyzes the simulation results, and Section 6 summarizes the research findings.

2. Establishment of the simulation framework

As illustrated in Fig. 1, the structure of the microscopic traffic flow simulation model comprises three main components: the initialization configuration unit, the vehicle motion model, and the data processing and analysis. Within the initialization configuration unit, the simulation scenario is meticulously defined, encompassing the initialization processes for both traffic and roadway parameters. The vehicle motion model is employed to depict behaviors such as lane-changing and the generation of vehicle trajectories over time. In the data processing and analysis stage, the traffic flow characteristics are extracted based on the spatio-temporal trajectories of the vehicles, enabling the evaluation of traffic flow operations.

2.1. Initialization of layout and vehicles

The initialization includes the setup of road layout and vehicle generation. Regarding the initialization configuration of the road environment, a ring road of length L is utilized as the testing ground to control traffic density on the arterial during simulation, as depicted in Fig. 2. The distance D_i between adjacent access points, such as $i-1$ and i, determines their traffic spacing along the ring road. The average spacing μ_d between access points is computed as the ratio of the ring road length L to the total number of traffic points N. The coefficient of variation c_v is uniformly applied to adjust the variability of access spacing. Without loss of generality, the initial traffic point is consistently positioned at 0. Consequently, the locations of all access points are individually determined using a normal distribution with a mean of μ_d and a standard deviation of $\mu_d c_v$. Specifically, when the variance is 0, access points are equally spaced along the ring road.

For the initialization of vehicle generation, two types of vehicles are considered: arterial and access vehicles. Initially, the arterial vehicles are evenly distributed on the ring road, and their states are subsequently updated based on the vehicle motion model outlined in Section 2.2. The total access traffic flow Q_A, is uniformly distributed among N access points. The arrival and exit of access vehicles are uniform to prevent the continuing increase of the traffic flow density on the ring road. Vehicles appear according to a Poisson distribution $P(\lambda)$ with an average flow rate of $\lambda = \frac{Q_A}{N}$ at each access point. Simultaneously, vehicles are randomly designated to exit the ring road from the nearest access point.

2.2. Vehicle motion model

Vehicle trajectories are primarily determined by the car-following model and the lane-changing model. Movements of vehicles within the same lane are elucidated by the car-following model, which encompasses three scenarios: free driving, car-following, and braking. When a vehicle indicates the intention to change lanes, its actions are governed by the lane-changing model, which involves lane-changing decision-making and execution. In the experiment, subject vehicles continually update their positional and speed states using the vehicle motion model. This iterative process relies on information concerning the positions and speeds of both the subject vehicles and neighboring vehicles (those ahead in the same lane, as well as the leading and trailing vehicles in the target lane). This iterative process unfolds at each time step to generate comprehensive vehicle trajectories. The specific vehicle motion model stands as the cornerstone of the entire microscopic traffic flow simulation. Further elaboration on this model will be provided in Section 3.

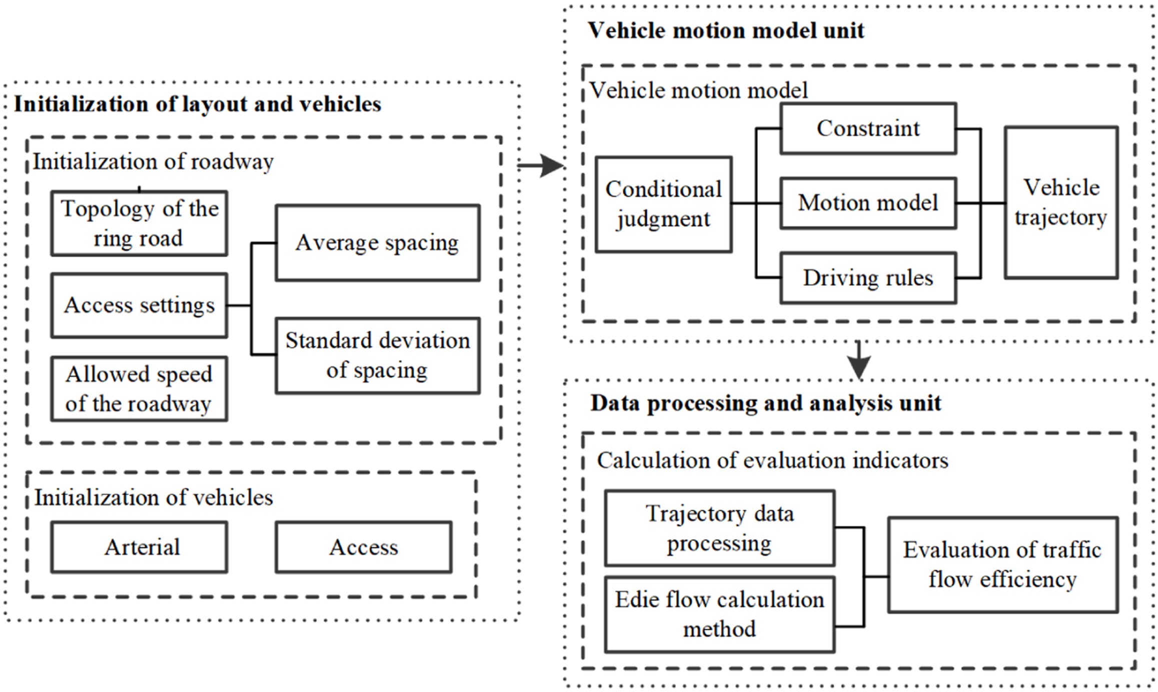

Fig. 1. Structure of the microscopic traffic flow simulation.

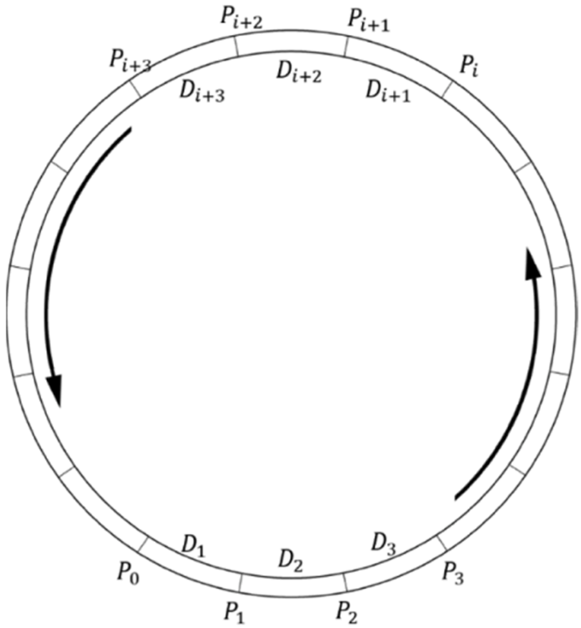

Fig. 2. Sketch of topological structure of ring road in simulation.

2.3. Data processing and analysis

To analyze the impact of access traffic on the arterial flow, measuring the traffic flow rate and density is essential. The flow rate within a specific period is calculated as the total distance covered by all vehicles during that time divided by the product of the duration of the period and the length of the road. Similarly, the average density within a specific period is computed as the total travel time of all vehicles during that time, divided by the product of the duration of the period and the length of the road. The formulas for flow rate and density are illustrated in Eqs. (1) and (2), respectively.

$$q(i) = \frac{d_V(i)}{LT} \tag{1}$$

$$k(i) = \frac{T_V(i)}{LT} \tag{2}$$

where $q(i)$ is the arterial traffic flow rate in period i, veh/h; $d_V(i)$ is the total distance travelled by all counted vehicles on the arterial in period i, km; L is the length of the ring road, km; T is the duration of the period, h; $k(i)$ is the average density of the arterial in period i, veh/km; and $T_V(i)$ is the total travel time in period i, h.

3. Microscopic traffic flow model

The microscopic traffic flow model constitutes the central component of the aforementioned microscopic traffic flow simulation framework. Vehicles can generate trajectories over time based on the car-following and lane-changing models ([29,41]b). In the subsequent section, the car-following and lane-changing models will be developed independently to depict the interactions between the access and arterial traffic.

3.1. Car-following model

This section is dedicated to constructing the car-following model based on the various driving states of vehicles. Our car-following model is constructed based on the Newell [28] car-following model, chosen for its simplicity and extensive utilization within microscopic traffic flow studies ([38,40]a; [48]). In this context, the position and speed of vehicle n at time t are denoted by $x_n(t)$ and $v_n(t)$, respectively. The reaction time of vehicle n is represented as τ_n. The states of free driving, car-following, deceleration, and braking are delineated by assessing the relationship between the subject vehicle and the leading vehicle at time $t + \tau_n$. The specific modeling methodology is outlined below.

3.1.1. Free driving

In scenarios where the traffic density on the road is low, signifying ample spacing between vehicles (exceeding the sum of the maximum distance $L_n(\tau_n)$ traveled within τ_n seconds and the minimum safe distance d_n), the subject vehicle will aim to achieve a higher travel speed until reaching the maximum. The progression of position and speed for vehicles in the free driving state is depicted by Eqs. (3) and (4) respectively.

$$x_n(t+\tau_n) = x_n(t) + L_n(\tau_n), \quad \forall x_{n-1}(t) - x_n(t) \in [L_n(\tau_n) + d_n, +\infty] \tag{3}$$

$$v_n(t+\tau_n) = \min(v_n(t) + \tau_n a_{max}, v_{max}), \quad \forall x_{n-1}(t) - x_n(t) \in [L_n(\tau_n) + d_n, +\infty] \tag{4}$$

$$L_n(\tau_n) = \min\left(v_{max}\tau_n, v_n(t)\tau_n + \frac{1}{2}a_{max}{\tau_n}^2\right) \tag{5}$$

where $x_n(t)$ represents the position of vehicle n at time t, m; τ_n is the reaction time of vehicle n, s; $L_n(\tau_n)$ is the maximum distance travelled by vehicle n within τ_n seconds, m, which can be calculated by Eq. (5); d_n is the minimum safe distance between vehicle n and the leading vehicle, m; v_n is the speed of vehicle n at time t, m/s; v_{max} is the maximum speed of the vehicle, m/s; and a_{max} is the maximum acceleration of the vehicle, m/s^2. Refer to previous literature, the maximum speed of the vehicle (v_{max}) is set at 50 km/h, the maximum and minimum accelerations ($a_{\max}$ and $a_{\min}$), which are set to be 5 and -5 m/s^2 [23], the minimum safe distance (d_n) is set as 12.5 m, and the reaction time (τ_n) for each driver is designated as 1.5 s [1].

3.1.2. Car-following

When the distance between the subject vehicle and the leading vehicle is greater than the minimum safe distance d_n, but less than the sum of the maximum distance $L_n(\tau_n)$ traveled within τ_n seconds and the minimum safe distance d_n, the subject vehicle will adapt its position and speed according to those of the leading vehicle, as illustrated by Eqs. (6) and (7) respectively.

$$x_n(t+\tau_n) = x_{n-1}(t) - d_n, \quad \forall x_{n-1}(t) - x_n(t) \in [d_n, L_n(\tau_n) + d_n) \tag{6}$$

$$v_n(t+\tau_n) = \frac{x_{n-1}(t) - x_n(t) - d_n}{\tau_n}, \quad \forall x_{n-1}(t) - x_n(t) \in [d_n, L_n(\tau_n) + d_n) \tag{7}$$

3.1.3. Deceleration and braking

During the merging of access vehicles onto the arterial, the distance between two vehicles may decrease to a point smaller than the minimum safe distance d_n of the rear vehicle. To prevent the rear vehicle from reversing, a phenomenon noted in the application of the Newell model in such scenarios, the model permits the rear vehicle to achieve maximum acceleration, facilitating the vehicle to rapidly decelerate to a stop. The progression of vehicle position and speed is delineated by Eqs. (8) and (9) respectively.

$$x_n(t+\tau_n) = x_n(t) + \frac{v_n(t)^2}{2a_{\min}}, \quad \forall x_{n-1}(t) - x_n(t) \in [0, d_n) \tag{8}$$

$$v_n(t+\tau_n) = 0, \quad \forall x_{n-1}(t) - x_n(t) \in [0, d_n) \tag{9}$$

where $a_{\min}$ is the minimum acceleration of the vehicle in the simulation, m/s^2.

3.2. Lane-changing model

The lane-changing behavior of vehicles is predominantly influenced by lane-change decision-making and acceptable gap assessment. On the one hand, evaluating lane change decisions involves computing the probability of the subject vehicle opting to remain in the current lane or switch to the target lane. This decision is based on factors such as spacing, speed, and other conditions between the subject vehicle and the leading and rear vehicles in both the current and target lanes. On the other hand, acceptable gap assessment involves determining whether there are appropriate gaps in the target lane for a vehicle to initiate a lane change when necessary.

3.2.1. Lane-changing decision model

Lane-changing demands emerge either to achieve higher speeds or to accomplish travel objectives while driving, like exiting the arterial by transitioning to the outermost lane. We assume that vehicle n has J available lanes to select from while driving. The utility of choosing lane j is denoted as U_{nj}. Following random utility theory, the lane-changing utility function U_{nj} can be constructed from deterministic factors influencing lane-changing decisions and an additive error term conforming to the Gumbel distribution, as illustrated in Eq. (10).

$$U_{nj} = V_{nj} + \varepsilon_{nj} \tag{10}$$

where U_{nj} is the utility of vehicle n choosing lane j; V_{nj} is the utility fixed term of vehicle n in choosing lane j; and ε_{nj} is the random error term that vehicle n in choosing lane j.

Whether a vehicle performs a lane change or not can be determined through Discrete Choice Theory (DCT), as depicted in Eq. (11). The essence of model construction lies in determining the fixed utility term V_{nj}, typically represented in a linear form as illustrated in Eq. (12).

$$P_{nj} = \frac{1}{1 + e^{-V_{nj}}} \tag{11}$$

where P_{nj} is the probability that vehicle n chooses lane j.

$$V_{nj} = \beta_0 + \sum_{k=1}^{K} \beta_k X_{njk} \tag{12}$$

where $\boldsymbol{\beta} = [\beta_0, \ldots, \beta_K]$ is the parameter vector that needs to be determined; $\boldsymbol{X_{nj}} = [X_{nj1}, \ldots, X_{njK}]^T$ is the characterization vector of choosing lane k for the subject vehicle; K is the number of characterization variables.

In the literature, many influencing factors are analyzed [52], such as the type of the leader vehicle [51], type of the subject vehicle [35], lateral distance [21], driver characteristics [36,37], traffic condition (speed and density differences) in adjacent lanes [30,54], vehicle-driver heterogeneity [22], and connected environment [3]. Among these factors, the distance and speed difference between the two leading vehicles in the target and current lanes are the primary factors [12,37].

In this study, the distance ΔD_{nj} between the two leading vehicles in the target lane and the current lane, and the speed difference Δv_{nj} between the two leading vehicles, are selected as the influencing factors that impact the subject vehicle's decision to change lanes. Trajectory data from the NGSIM dataset on Lankershim Boulevard with the time range between 08:30 and 09:00 [2,4,15,32] is utilized to calibrate the parameters of the lane-changing decision model using the maximum likelihood function estimation method. The running information of vehicles is extracted using the following steps.

Step 1: Chunk the vehicles according to the Frame_ID, and extract the relevant information corresponding to the vehicles frame by frame.
Step 2: Judge whether the vehicle changes lanes according to whether the lane number is altered, adding a new category attribute Ch, and changing lanes, then Ch = 1, otherwise Ch = 0.
Step 3: Filter the vehicle data information in a specific video image frame where Int_ID equals 0 (no near intersections), and V_Class equals 2 (small car).
Step 4: Determine the front and rear vehicle numbers and positions of the vehicle as well as the positions of the leading and trailing vehicles in the target lanes based on the longitudinal position of the vehicle, Local_Y. Then, the parameters related to distance can be obtained.
Step 5: Obtain parameters related to speed based on the target vehicle number and the corresponding speed information of the vehicle in the neighboring lanes.
Step 6: Repeat the computation process of Steps 4 and 5 until all eligible vehicle information in the current frame is screened, then switch to the next frame.
Step 7: Output the vehicle data information that satisfies the conditions after screening.

The calibration results of the parameter vector $\boldsymbol{\beta}$ are presented in Table 1. The goodness of fit, with $\rho^2 = 0.342 > 0.2$, signifies a high level of accuracy [17]. The significance p-values for the vectors ΔD_{nj} and Δv_{nj} are below 0.05, indicating that these variables significantly influence whether a vehicle opts to change lanes. The calibrated parameter values show that the probability of a vehicle changing lanes is positively associated with the relative values of the distance and speed between the two leading vehicles. This implies that a greater spacing between the leading vehicles in the target and current lanes, or a more significant speed difference, increases the likelihood of a lane change. This observation aligns with our general understanding. Based on the calibration outcomes, the utility function for lane-changing decisions is represented in Eq. (13).

$$V_{nj} = -0.469 + 0.018\Delta D_{nj} + 0.058\Delta v_{nj} \tag{13}$$

where ΔD_{nj} is the distance between the two leading vehicles in the target lane and the current lane, m; Δv_{nj} is the speed difference between the two leading vehicles in the target lane and the current lane, m/s.

3.2.2. Gap acceptance model

When a vehicle initiates a lane-changing request, the feasibility of gaps for lane changes is established by assessing the size of the gaps or velocities between the subject vehicle and the leading and trailing vehicles in the target lane. Similar to the lane-changing decision model, the evaluation of gap acceptability can also be elucidated through DCT, as depicted in Eq. (14).

Table 1
Calibration results of lane-changing decision model.

Variables	Parameters	Values	t-value	Significance
ΔD_{nj}	β_1	0.018	2.121	0.034
Δv_{nj}	β_2	0.058	3.235	0.015
Constant	β_0	-0.469	-3.132	0.005
Goodness of fit	0.342			

$$P_{ng} = \frac{1}{1 + e^{-V_{ng}}} \tag{14}$$

where P_{ng} and V_{ng} are the probability and the utility fixed term that vehicle n accepts the gap, respectively.

We consider the speed v_n of the subject vehicle, the speed difference Δv_{nF} between the subject vehicle and the leading vehicle in the target lane, and the speed difference Δv_{nL} between the subject vehicle and the rear vehicle in the target lane as the influencing factors affecting the vehicle's decision to accept a gap. Trajectory data extracted from the NGSIM dataset is utilized to calibrate the paforementioned gap acceptance model parameters hrough maximum likelihood function estimation. The calibration results of the parameter vector $\boldsymbol{\beta}$ are presented in Table 2, indicating a high level of accuracy with a goodness of fit of $\rho^2 = 0.294 > 0.2$ [17]. Regarding v_n, Δv_{nF} and Δv_{nL}, the significance p-value is below 0.05, signifying that these variables significantly influence the subject vehicle's acceptance of the gap. Analysis of the calibrated parameter values reveals a negative correlation between the probability of gap acceptance and the speed of the subject vehicle and the speed difference between the subject vehicle and the leading vehicle in the target lane. In contrast, a positive correlation is observed with the speed difference between the subject vehicle and the rear vehicle in the target lane. This suggests that a more minor speed difference between the subject vehicle and the leading vehicle in the target lane or a more significant speed difference between the subject vehicle and the rear vehicle in the target lane increases the likelihood of gap acceptance. This observation aligns with a common understanding. Based on the calibration results, the utility function of gap acceptance is delineated in Eq. (15).

$$V_{nj} = -2.241 - 0.064 v_n - 0.136 \Delta v_{nF} + 0.083 \Delta v_{nL} \tag{15}$$

where v_n is the speed of vehicle n, m/s; Δv_{nF} is the speed difference between the subject and the leading vehicle of the target lane, m/s; Δv_{nL} is the speed difference between the subject and the rear vehicle of the target lane, m/s.

4. Simulation experiment design

Drawing upon the aforementioned microscopic traffic flow simulation framework and the car-following and lane-changing models, the operational dynamics of road traffic flow can be effectively simulated across various access traffic arrangement scenarios. This section aims to delineate the specific scenarios slated for testing within the simulation, along with the requisite duration for each scenario to be evaluated.

4.1. Simulation test setting

A two-lane ring road with a length of $L = 10.5$ km is chosen, as illustrated in Fig. 3. To account for variances in vehicle speeds when entering and exiting the arterial, the speeds of vehicles entering the arterial from the access points are randomly selected within the range of 10–15 km/h, while the speeds of vehicles exiting from the arterial are randomly reduced to 5–10 km/h.

Simulation experiments are configured with varying access spacing scenarios, focusing on the performance evaluation of four key parameters: arterial traffic density k, traffic demand intensity C of access, average spacing of access points μ_d, and variation coefficient c_v of access spacing. Specifically, the arterial traffic density is sampled at intervals of $\frac{1}{40d}$, where $d = 12.5$ represents the minimum safe distance between vehicles, resulting in a total of forty values. The traffic demand intensity of access is considered in increments of 50 veh/h/km within the range of 50 veh/h/km to 600 veh/h/km, comprising a total of six values. Adhering to the minimum access spacing stipulated at 150 m in the Urban Residential Area Planning and Design Standards [27], the average spacing of access points varies from 1/6 of the minimum value to 20 times that value, encompassing seven values. The variation coefficient of access spacing is set at 0 (equal spacing), 0.1, and 0.2, leading to a total of three values. The specific values for these parameters are detailed in Table 3. Considering the permutations of these parameters, a total of $40 \times 6 \times 7 \times 3 = 5040$ distinct working conditions are subjected to testing.

4.2. Simulation duration analysis

Given the inherent randomness in the simulation process, conducting sufficient simulation runs with sufficient durations is imperative to ensure result stability. In this section, the capacity (maximum flow) is utilized as an indicator to assess changes in road capacity across different simulation durations. The initial settings for the simulation in Fig. 4 include an access traffic demand intensity of $C = 150$ veh/h/km, an average spacing of access points at $\mu_d = 150$ m, and a variation coefficient of $c_v = 0$. 10 simulations are

Table 2
Calibration results of gap acceptance model.

Variables	Parameters	Values	t-value	Significance
v_n	β_1	-0.064	-2.452	0.013
Δv_{nF}	β_2	-0.136	1.862	0.026
Δv_{nL}	β_3	0.083	-3.658	0.008
Constant	β_0	-2.241	-3.542	0.002
Goodness of fit	0.294			

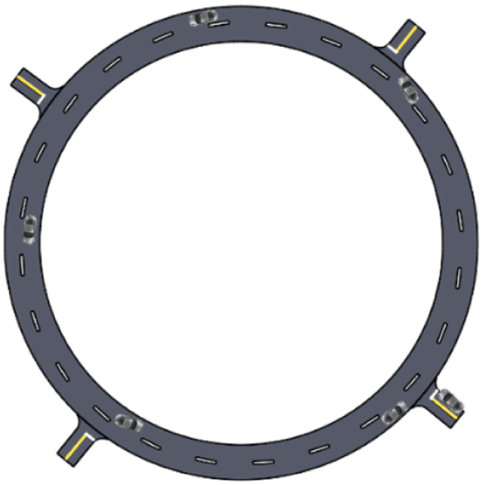

Fig. 3. Schematic diagram of simulation environment.

Table 3
Parameter and values.

Parameters	Values						
k	$\frac{1}{40}k_j$	$\frac{2}{40}k_j$	$\frac{3}{40}k_j$	…	$\frac{38}{40}k_j$	$\frac{39}{40}k_j$	k_j
C	50	100	150	300	450	600	
μ_d	25	75	150	300	500	1000	1500
c_v	0	0.1	0.2				

conducted for the same duration and the outcomes are depicted in Fig. 4. The average capacity value tends to stabilize when the simulation duration is 70 min. Therefore, in the ensuing analysis, one simulation run with a consistent duration of 70 minutes was performed for each working condition.

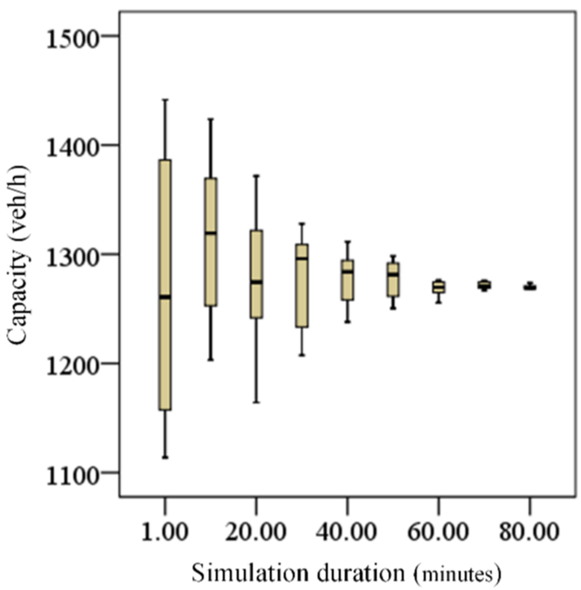

Fig. 4. Relationship between calculation stability of capacity and simulation time.

5. Results analysis

This study aims to investigate the overall impact of different arrangements of access traffic on arterial roads. It is a macro-level issue. Therefore, we analyze macroscopic traffic flow in the hereafter analysis. According to the simulation experiment results, flow-density and speed-density curves are generated to represent traffic flow trends visually and driving speed across various scenarios. These plots serve to elucidate the impact of access traffic on arterial capacity. Subsequently, an analysis can be conducted to summarize how access traffic influences the overall capacity of the arterial road.

5.1. Traffic flow and speed curve variation analysis

We analyze the flow-density and speed-density curves of the arterial road network for two specific scenarios. These scenarios are outlined as follows: (1) the operational condition featuring the average spacing of all access points under an access traffic demand intensity of $C = 150$ veh/h/km and a variation coefficient of $c_v = 0$; (2) the operational condition characterized by access traffic demand with an average spacing of access points at $\mu_d = 300$ m and a variation coefficient of $c_v = 0$. The curves illustrating the variations of traffic flow and speed concerning arterial traffic density are presented in Fig. 5.

Access points' average spacing and demand notably impact arterial traffic flow and speed. Generally, a larger spacing for access points or higher demand for access traffic results in lower arterial traffic flow and speed.

The relationship between flow and density for various access spacings is illustrated in Fig. 5(a). When the density is below 20 veh/km, there is no significant disparity in traffic flow among different access spacings. This indicates that access spacing minimizes arterial traffic flow at lower traffic volumes. However, as the density increases, variances between the flow curves within the clusters become apparent. The curves are organized from top to bottom based on the ascending order of access spacing, indicating that smaller access spacings have a lesser impact on arterial traffic flow and yield higher values.

The relationship between flow and density for various access traffic demands is depicted in Fig. 5(b). When the density is below 20 veh/km, there is no significant distinction in traffic flow among different access traffic demand curves. This indicates that access traffic demand minimally influences arterial traffic flow at lower traffic volumes. However, as the density increases, variances between the flow curves within the clusters start to emerge. The curves are ordered from top to bottom based on increasing access traffic demand, revealing that more minor access traffic demands have a lesser impact on arterial traffic flow and higher arterial flow values.

Figs. 5(c) and (d) illustrate the relationship between speed and density. The general trend aligns with Figs. 5(a) and (b).

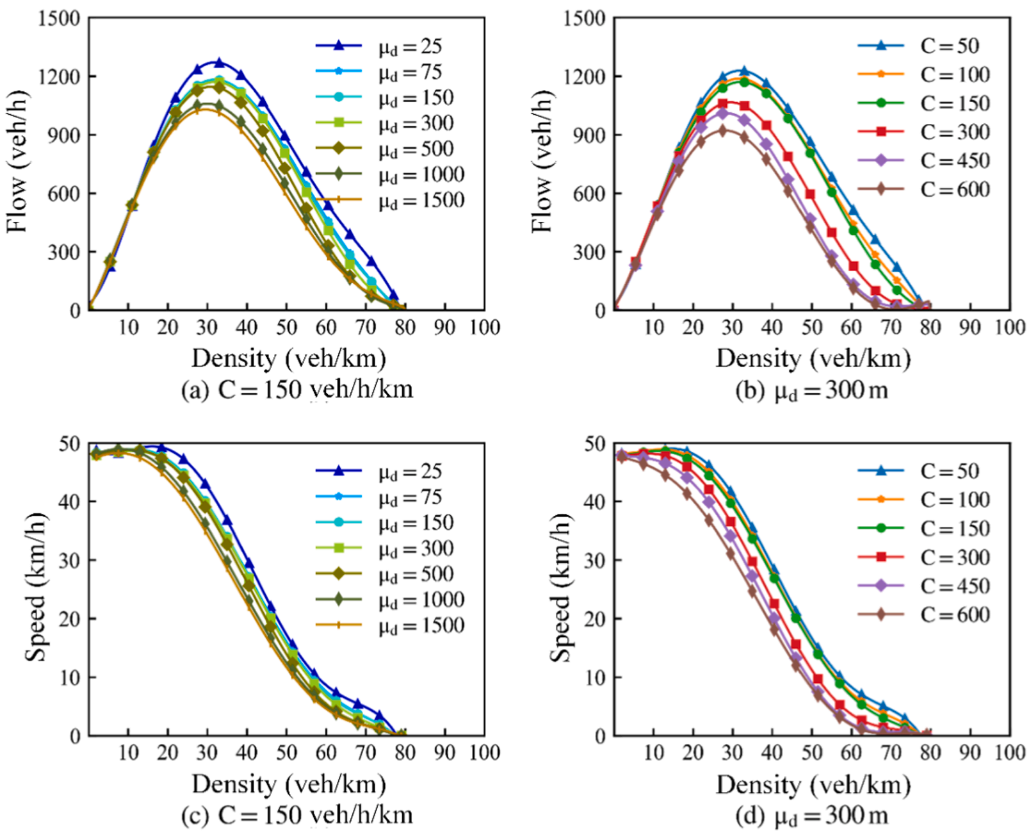

Fig. 5. Traffic flow and speed variation curves with arterial density.

Specifically, a smaller access spacing or lower traffic demand for access corresponds to higher arterial operating speeds.

The flow-density curves for all the remaining cases with a variation coefficient $c_v = 0$ of access points are presented in Fig. 6. These curves can lead to conclusions that are consistent with the observations mentioned above.

5.2. Impact analysis of capacity

Fig. 7 illustrates the variation of the maximum flow (capacity) of the traffic flow with the average spacing of the access points, considering different combinations of access traffic demands and variation coefficients of access spacing. In the figure, lines representing the same values of access traffic demand intensity C are depicted in the same color, with three types of variation coefficients of access spacing $c_v = 0.0,\ 0.1,\ 0.2$ represented by solid, dotted, and dashed lines respectively.

We observe a close relationship between capacity and the traffic demand intensity of access, as well as the average spacing of access points. There exists a negative correlation between capacity and both of these factors. Specifically, the highest arterial traffic flow is obtained when the interference from access traffic is at its lowest. For the traffic demand intensity of access, it has the most minor effect on arterial traffic at its minimum value. As the traffic demand intensity of access increases, the capacity decreases.

Furthermore, as the average spacing of access points increases, the disparities between capacities under different access traffic demands also grow. This suggests that in the trade-off between the traffic volume of access and the traffic demand at a single access point, the traffic demand at the single access point exerts a more significant influence on the capacity of arterial traffic flow. When considering a fixed total traffic demand of access, increasing the number of access points diminishes the arterial traffic capacity. The impact of the average spacing of access points (μ_d) on arterial capacity becomes apparent only after μ_d exceeds 150m. The change in traffic capacity under different spacing between access points is susceptible to the traffic demand intensity of access (C). When $C = 50$ veh/h/km, the traffic capacity decreases by only 6 % as μ_d increases from the minimum value to 1500 m. However, when $C = 600$, the traffic capacity decreases by 66 % as μ_d increases from the minimum value to 1500 m. The impact of average spacing of access points on traffic capacity increases by about 12 % for every 50 veh/h/km increase in the traffic demand intensity of access.

This intriguing finding, derived from microscopic simulation, challenges the conventional wisdom prevalent in past planning practices where a greater average spacing of access points was believed to enhance the service level of arterials. This shift in understanding primarily stems from the assumption of a fixed total demand of access traffic on the arterial. In the simulation experiment, maintaining constant access traffic demand implies that the traffic demand at individual access points increases with the larger average spacing of access points. However, in the planning scenarios, inadequate spacing of access points necessitates establishments to position access points on intersecting or parallel roads to meet minimum requirements. Essentially, it redistributes the traffic demand for access.

6. Conclusions

This study examines the impact of right-in-right-out access traffic on the operation of arterial traffic flow using microscopic traffic dynamic simulation. A microscopic traffic flow simulation model resembling a ring road is constructed to regulate arterial traffic density in the simulation. The macroscopic traffic flow states are inferred through microscopic car-following and lane-changing models. The following motion encompasses free driving, car-following, and deceleration and braking. Lane-changing motion involves considerations of lane-changing decisions and acceptable gaps. The experimental scenarios encompass four influencing factors: arterial traffic density, traffic demand intensity of access, average spacing of access points, and variation coefficient of access spacing. Through testing the flow and speed of the ring arterial under 5040 operational conditions (equivalent to 5880 simulation hours), the impact of access traffic on arterial traffic capacity and speed is visually represented via a series of flow-density and speed-density curves. The simulation experiments are analyzed, and the following findings can be obtained:

(1) The probability of a vehicle opting for a lane change is positively correlated with a larger spacing between the two leading vehicles in the target lane and the current lane, as well as a more significant speed difference between them (both with significance *p*-values below 0.05). Conversely, a higher likelihood of accepting a gap is associated with a minor speed difference between the subject vehicle and the leading vehicle of the target lane or a more significant speed difference between the subject vehicle and the rear vehicle of the target lane (both with significance *p*-values below 0.05).

(2) The impact on arterial traffic flow increases with a larger average spacing of access points, as revealed in this intriguing finding from microsimulation. When the total traffic demand enters and exits the arterial remains constant, excessive spacing between access points leads to traffic overloading at individual access points, ultimately diminishing the arterial capacity. Conversely, in scenarios with a fixed total traffic demand for entering and exiting the arterial, a smaller spacing between access points enhances the traffic capacity of the arterial. This observation aligns with the outcomes of prior theoretical and simulation studies concerning the influence of crosswalks on vehicular flow [8,20].

(3) At low levels of arterial traffic volume, access exerts minimal to no influence on arterial traffic flow. However, as the traffic demand intensity for access increases (more than 150 veh/h/km), the impact on arterial traffic flow becomes more pronounced, leading to reductions in both capacity and speed.

One of the limitations of the study is that it only explores the trends through extensive simulation. Due to the difficulties in conducting comparative experiments in reality, it might be necessary to compare two roads with similar road geometry and traffic

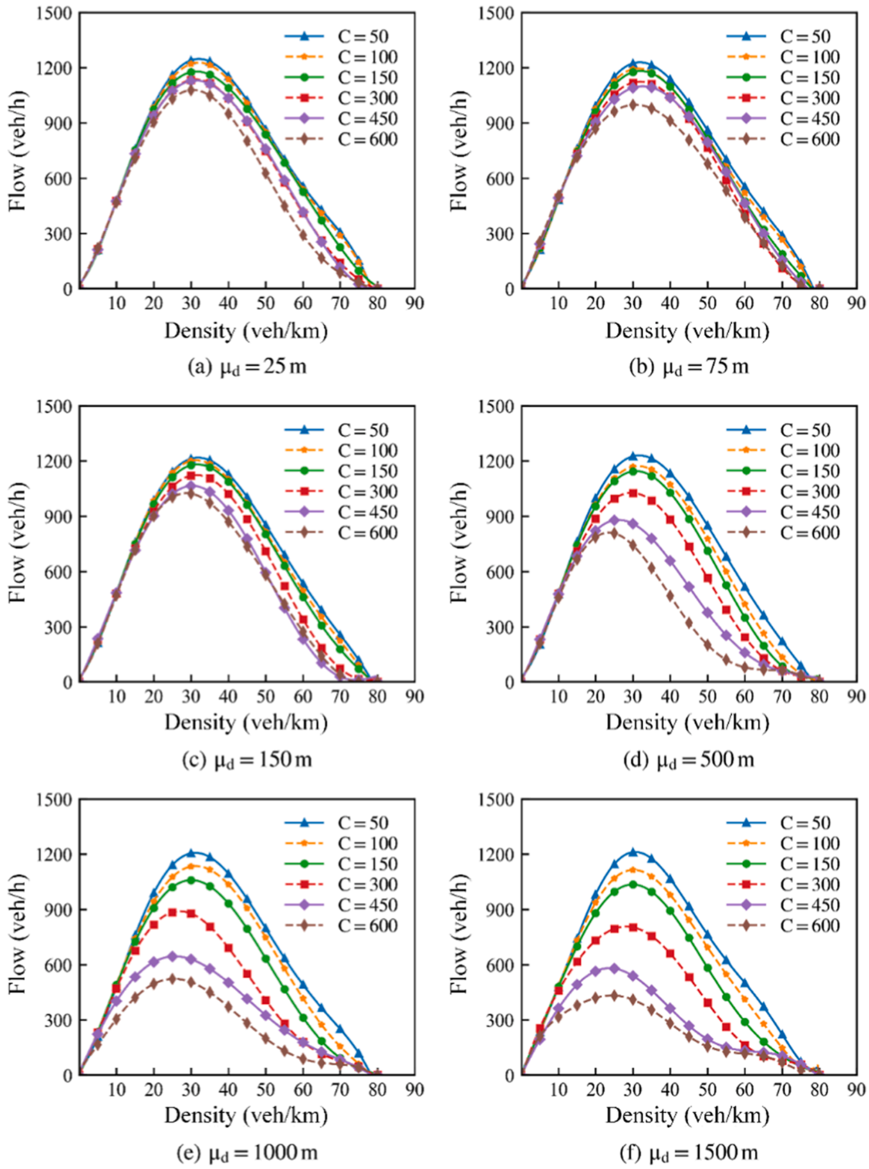

Fig. 6. Traffic flow-density curve for the case of variation coefficient $c_v = 0$ of access spacing.

demand in the same area with different access management methods. If suitable conditions arise, analyzing the data using actual data would be an exciting research direction. Besides, the benefits analysis of different access point optimization strategies can be strengthened. The study does not discuss access point optimization strategies, which may include auxiliary lanes, yield rules, yield signs, and the integration of connected vehicles. Future research can evaluate the benefits through comprehensive large-scale simulation experiments and quantify the effect of each design intervention measure in reducing the impact of traffic on the arterial system.

CRediT authorship contribution statement

Jing Zhao: Conceptualization, Methodology, Software, Writing – original draft, Writing – review & editing. **Yulan Xia:** Software, Data curation, Writing – original draft, Writing – review & editing, Visualization. **Chaojun Wang:** Methodology, Validation, Writing – original draft, Writing – review & editing. **Jairus Odawa:** Validation, Writing – review & editing.

Declaration of competing interest

The authors declare that they have no known competing financial interests or personal relationships that could have appeared to influence the work reported in this paper.

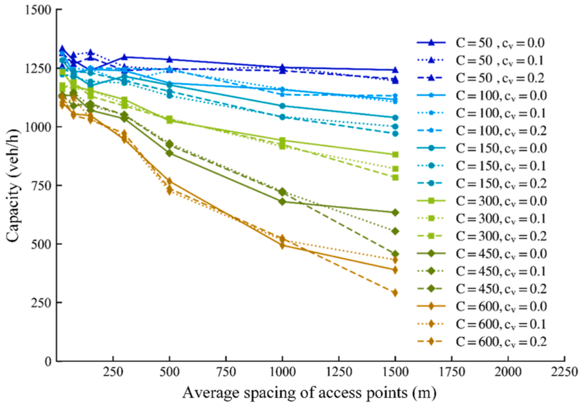

Fig. 7. Impacts of access spacing arrangement on arterial capacity.

Acknowledgements

This work was supported by the National Natural Science Foundation of China [grant numbers 52122215 and 52372304] and Shanghai Shuguang Program [grant number 22SG45].

Data availability

Data will be made available on request.

References

[1] S. Ahn, M.J. Cassidy, J. Laval, Verification of a simplified car-following theory, Methodological 38 (2004) 431–440.
[2] Y. Ali, Z. Zheng, M.C.J. Bliemer, Calibrating lane-changing models: Two data-related issues and a general method to extract appropriate data, Emerg. Technol.s 152 (2023) 104182.
[3] Y. Ali, Z. Zheng, M.M. Haque, M. Wang, A game theory-based approach for modelling mandatory lane-changing behaviour in a connected environment, Emerg. Technol. 106 (2019) 220–242.
[4] Y. Ali, Z. Zheng, M.M. Haque, M. Yildirimoglu, S. Washington, Detecting, analysing, and modelling failed lane-changing attempts in traditional and connected environments, Anal. Methods Accid. Res. 28 (2020) 100138.
[5] T.P. Barrette, J. Warner, P. Thompson, P.T. Savolainen, Access separation at interchanges: examining crash rates on the cross-street and in the transition areas from full to partial access control, Transp. Res. Rec. 2672 (2018) 1–10.
[6] M.A. Brewer, K. Fitzpatrick, J.C. Cline, Driveway access spacing considerations for rural highways with high truck volumes, Transp. Res. Rec. 2674 (2020) 477–490.
[7] C.M. Chu, H. Nathan, C. Mashrur, H.O. Jennifer, A.S. Wayne, J.D. William, Impact of minimum driveway spacing policies on safety performance: An integrated traffic micro-simulation and automated conflict analysis, Internat. J. Transport. Sci. Techn. 3 (2014) 249–264.
[8] C.F. Daganzo, V.L. Knoop, Traffic flow on pedestrianized streets, Methodological 86 (2016) 211–222.
[9] K.K. Dixon, L.S. Brown, Assessing how drivers of through vehicles react to driveway activity, Transp. Res. Rec. 2404 (2014) 77–84.
[10] Y. Du, C. Zhao, X. Zhang, L. Sun, Microscopic simulation evaluation method on access traffic operation, Simul. Model. Pract. Theory. 53 (2015) 139–148.
[11] J.L. Gattis, J.R. Chimka, A. Evans, Access spacing based on turning-vehicle acceleration, Transp. Res. Rec. 2618 (2017) 1–7.
[12] P.G. Gipps, A model for the structure of lane-changing decisions, Methodological 20 (1986) 403–414.
[13] J.S. Gluck, G. Haas, J. Mahmood, H.S. Levinson, Driveway spacing and traffic operations, *Transport. Res. Circul.* E-C 019 (2000) C–3.
[14] R. Hamzeie, M.U. Megat-Johari, I. Thompson, T.P. Barrette, T. Kirsch, P.T. Savolainen, Examining safety on two-lane and multilane highways in consideration of access spacing, Transp. Res. Rec. 2673 (2019) 388–397.
[15] X. Hu, Z. Zheng, D. Chen, X. Zhang, J. Sun, Processing, assessing, and enhancing the Waymo autonomous vehicle open dataset for driving behavior research, Emerg. Techn. 134 (2022) 103490.
[16] B. Huang, Y. Zhang, L. Lu, J. Lu, A new access density definition and its correlation with crash rates by microscopic traffic simulation method, Accident Analy. Prevent. 64 (2014) 111–122.
[17] J.C. Kern, Introduction to regression analysis, Am. Stat. 61 (2007) 101. -101.
[18] S.M. Khan, J. Mitchell, M. Chowdhury, K. Dey, N. Huynh, Operational analysis of a connected vehicle-supported access control on urban arterials, Iet Intellig. Transport Syst. 12 (2018) 134–142.
[19] K.M. Kim, M. Saito, G.G. Schultz, D.L. Eggett, Evaluating safety impacts of access management alternatives with the surrogate safety assessment model, Transp. Res. Rec. 2672 (2018) 120–128.
[20] V.L. Knoop, C.F. Daganzo, The effect of crosswalks on traffic flow, Euro. J. Transport Infrastruct. Res. 18 (2018) 145–157.
[21] G. Li, L. Zhao, W. Tang, L. Wu, J. Ren, Modeling and analysis of mandatory lane-changing behavior considering heterogeneity in means and variances, Statist. Mech. Applic. 622 (2023) 128825.
[22] Q. Li, X. Li, F. Mannering, Assessment of discretionary lane-changing decisions using a random parameters approach with heterogeneity in means and variances, Transp. Res. Rec. 2675 (2021) 330–338.
[23] M. Liu, J. Zhao, S. Hoogendoorn, M. Wang, A single-layer approach for joint optimization of traffic signals and cooperative vehicle trajectories at isolated intersections, Emerg. Techn. 134 (2022) 103459.
[24] T. Mauga, M. Kaseko, Modeling and evaluating safety impacts of access management features in the Las Vegas, Nevada, Valley, Transp. Res. Rec. 2171 (2010) 57–65.
[25] A.I.M. Medina, F. Creemers, E. Lefeber, N. van de Wouw, Optimal access management for cooperative intersection control, IEEE Transact. Intellig. Transport. Syst. 21 (2020) 2114–2127.

[26] M.U. Megat-Johari, B. Bazargani, T.J. Kirsch, T.P. Barrette, P.T. Savolainen, An examination of the safety of signalized intersections in consideration of nearby access points, Transp. Res. Rec. 2672 (2018) 11–21.
[27] MOHURD, Standard for urban residential area planning and design. Ministry of housing and urban-rural development of the People's Republic of China, China Architecture & Building Press, Beijing, China, 2018.
[28] G.F. Newell, A simplified car-following theory: a lower order model, Methodological 36 (2002) 195–205.
[29] D. Ni, Limitations of current traffic models and strategies to address them, Simul. Model. Pract. Theory. 104 (2020) 102137.
[30] M. Park, K. Jang, J. Lee, H. Yeo, Logistic regression model for discretionary lane changing under congested traffic, Transport Sci. 11 (2015) 333–344.
[31] R.V. Ponnaluri, Y.D. Santhi, Road crash history and risk groups in India need for new initiatives and safety policies, Transp. Res. Rec. 2114 (2009) 64–71.
[32] V. Punzo, M.T. Borzacchiello, B. Ciuffo, On the assessment of vehicle trajectory data accuracy and application to the Next Generation SIMulation (NGSIM) program data, Emerg. Techn. 19 (2011) 1243–1262.
[33] G.G. Schultz, K.T. Braley, T. Boschert, Relationship between access management and other physical roadway characteristics and safety, J. Transp. Eng. 136 (2010) 141–148.
[34] G.G. Schultz, J.S. Lewis, T. Boschert, Safety impacts of access management techniques in Utah, Transp. Res. Rec. 1994 (2007) 35–42.
[35] S. Sharma, M. Snelder, L. Tavasszy, H. van Lint, Categorizing merging and diverging strategies of truck drivers at motorway ramps and weaving sections using a trajectory dataset, Transp. Res. Rec. 2674 (2020) 855–866.
[36] D. Sun, L. Elefteriadou, Lane-changing behavior on urban streets: an "in-vehicle" field experiment-based study, Comput.-Aided Civil Infrastr. Eng. 27 (2012) 525–542.
[37] D. Sun, L. Elefteriadou, A driver behavior-based lane-changing model for urban arterial streets, Transport. Sci. 48 (2014) 184–205.
[38] J. Sun, H. Liu, Z. Ma, Modelling and simulation of highly mixed traffic flow on two-lane two-way urban streets, Simul. Model. Pract. Theory. 95 (2019) 16–35.
[39] G. Tenekeci, N. Hansen, S. Wainaina, A. Mohammad, Integrated traffic management: benefit analysis of three layered approach, IET Intellig. Transp. Syst. 8 (2014) 665–680.
[40] J. Tian, C. Zhu, D. Chen, R. Jiang, G. Wang, Z. Gao, Car following behavioral stochasticity analysis and modeling: perspective from wave travel time, Methodological 143 (2021) 160–176.
[41] J. Tian, C. Zhu, R. Jiang, M. Treiber, Review of the cellular automata models for reproducing synchronized traffic flow, Transp. Sci. 17 (2021) 766–800.
[42] TRB, Driveway and street intersection spacing, Transport. Res. Circul. 456 (1996) 1–43.
[43] TRB, Highway capacity manual. A guide for multimodal mobility analysis, 6th edition, Transportation Research Board of the National Academy of Science, Washington, DC, 2016.
[44] K.M. Williams, V.G. Stover, K.K. Dixon, P. Demosthenes, Access management manual, Transportation Research Board, Washington, DC, USA, 2014.
[45] J. Xu, J.H. Lambert, C.J. Tucker, Highway access safety program evaluation with uncertain parameters, J. Transp. Eng. 140 (2014) 04013010.
[46] X. Yang, H. Zhou, CORSIM-based simulation approach to evaluation of direct left turn versus right turn plus U-turn from driveways, J. Transp. Eng. 130 (2004) 68–75.
[47] B. Zhang, H. Zhou, Access control techniques to mitigate wrong-way driving activities on multilane divided highways: Case studies in Alabama, Transp. Res. Rec. 2673 (2019) 745–754.
[48] D. Zhang, X. Chen, J. Wang, Y. Wang, J. Sun, A comprehensive comparison study of four classical car-following models based on the large-scale naturalistic driving experiment, Simul. Model. Pract. Theory. 113 (2021) 102383.
[49] J. Zhao, V.L. Knoop, J. Sun, Z. Ma, M. Wang, Unprotected left-turn behavior model capturing path variations at intersections, IEEE Transact. Intellig. Transport. Syst. 24 (2023) 9016–9030.
[50] J. Zhao, R. Ma, M. Wang, A behaviourally underpinned approach for two-dimensional vehicular trajectory reconstruction with constrained optimal control, Emerg. Techn. 159 (2024) 104489.
[51] J. Zheng, K. Suzuki, M. Fujita, Predicting driver's lane-changing decisions using a neural network model, Simul. Model. Pract. Theory. 42 (2014) 73–83.
[52] Z. Zheng, Recent developments and research needs in modeling lane changing, Methodological 60 (2014) 16–32.
[53] H. Zhou, K.M. Williams, W. Farah, Methodology to evaluate the effects of access control near freeway interchange areas, J. Transp. Eng. 134 (2008) 504–511.
[54] C. Zhu, S. Zhong, S. Ma, Two-lane lattice hydrodynamic model considering the empirical lane-changing rate, Comm. Nonlinear Sci. Numer. Simul. 73 (2019) 229–243.